Supplementary Information

Millisecond photonic sintering of iron oxide doped alumina ceramic coatings

Evgeniia Gilshtein[1+,*], Stefan Pfeiffer[2+,*], Marta D. Rossell[3], Jordi Sastre[1], Lovro Gorjan[2], Rolf Erni[3], Ayodhya N. Tiwari[1], Thomas Graule[2], Yaroslav E. Romanyuk[1,*]

[1] Laboratory for Thin Films and Photovoltaics, Empa – Swiss Federal Laboratories for Materi-als Science and Technology, Überlandstrasse 129, 8600 Dübendorf, Switzerland
[2] Laboratory for High Performance Ceramics, Empa – Swiss Federal Laboratories for Materi-als Science and Technology, Überlandstrasse 129, 8600 Dübendorf, Switzerland
[3] Electron Microscopy Center, Empa – Swiss Federal Laboratories for Materials Science and Technology, Überlandstrasse 129, 8600 Dübendorf, Switzerland

[+] Evgeniia Gilshtein and Stefan Pfeiffer contribute equally to this paper.

Keywords: Flash lamp annealing, Intense pulsed light, ceramic coating, alumina, iron oxide

Table S1. Absolute density and specific surface area (SSA) of raw powders measured by helium pycnomerty and BET measurements, respectively, and calculated BET average particle sizes for all powders.

	absolute density [g/cm^3]	SSA [m^2/g]	BET average particle size [nm]
Al_2O_3 AA3	4.01	0.40	3756
Al2O3 Taimicron TM-Dar	3.95	11.80	129
Fe_2O_3 L2715D	4.38	69.73	20

Table S2. d_{10}, d_{50} and d_{90} of volume based particle size distributions of dispersed powders in water determined by dynamic light scattering (DLS) and laser diffraction (LD).

Powder	Al_2O_3 AA3	Al_2O_3 Taimicron TM-DAR		Fe_2O_3 L2715D	
Measurement method	LD	LD	DLS	LD	DLS
d_{10}	2.2 µm	109 nm	133 nm	51 nm	37 nm
d_{50}	3.0 µm	148 nm	201 nm	79 nm	53 nm
d_{90}	4.4 µm	212 nm	295 nm	110 nm	82 nm

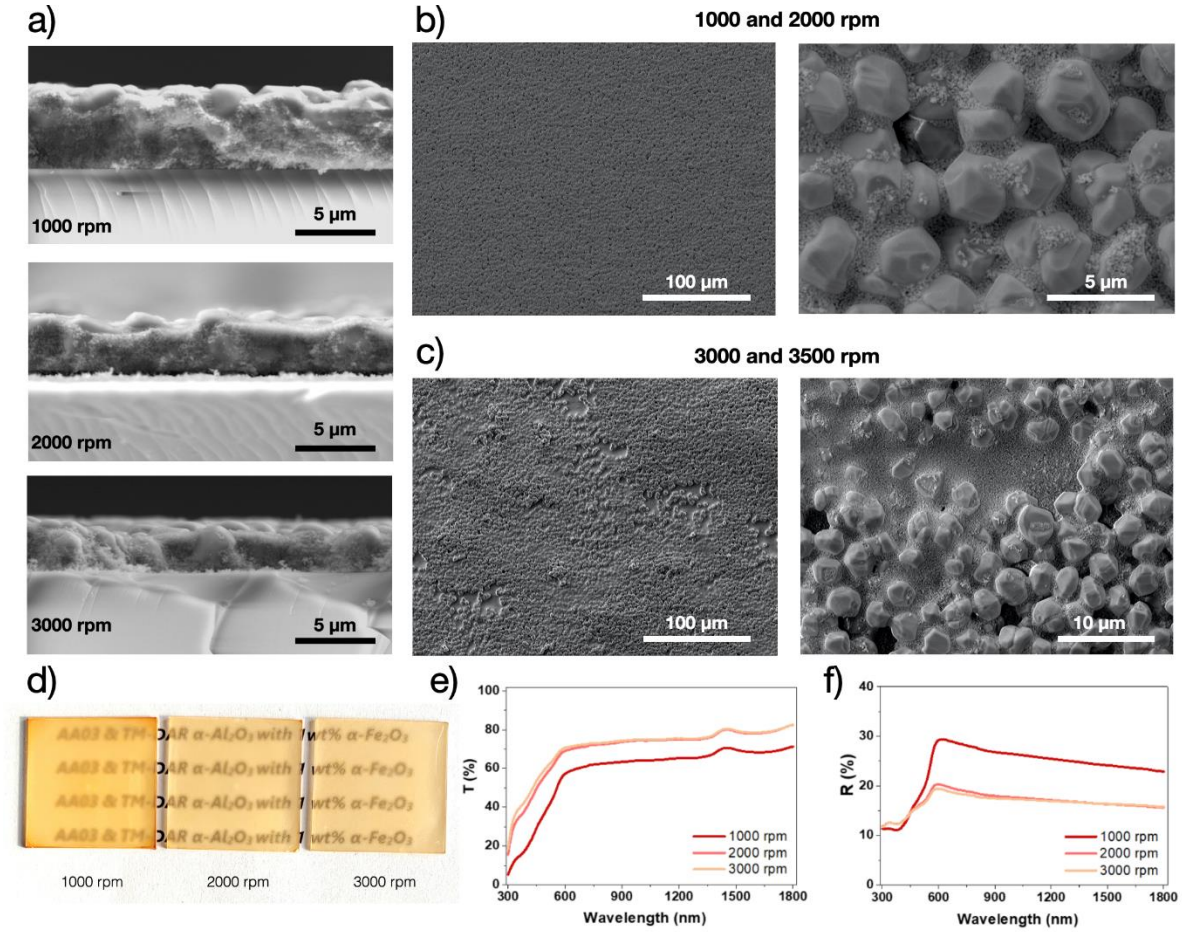

Supplementary Fig.1. Characterization of ceramic layers (α-Al_2O_3 bimodal mixture doped with 1wt% α-Fe_2O_3) fabricated by spin coating with different rotation speeds (from 1000, 2000, and 3000 rpm): a) cross-sectional SEM images, b) top-view SEM images revealing uniform coating with 1000 and 2000 rpm, c) top-view SEM images showing non-uniform coating at 3000 and above rpm used, d) Photographs of the spin coated layers, e) optical transmittance and f) reflectance spectra of the spin coated layers.

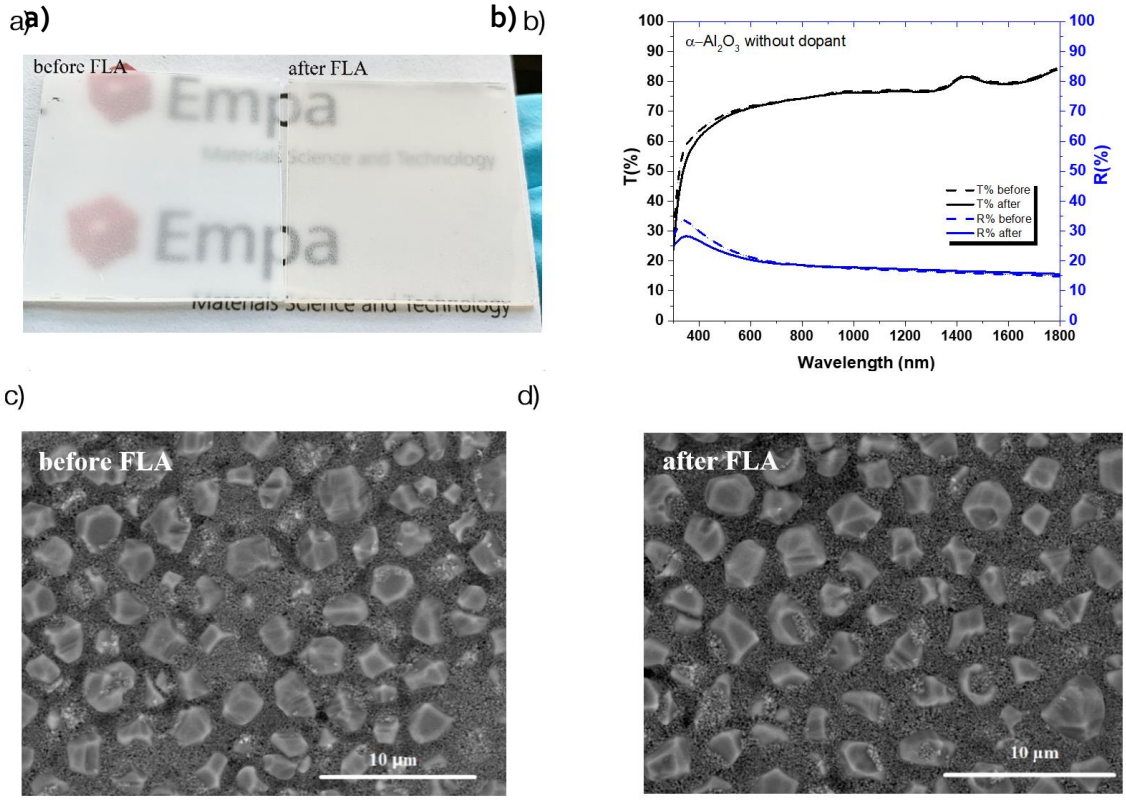

Supplementary Fig.2. Characterization of ceramic layers (α-Al_2O_3 bimodal mixture) without α-Fe_2O_3 dopant, before and after photonic sintering: top-view SEM images and optical transmittance and reflectance spectra. Photographs of the as-fabricated spin coated layer and layer after photonic sintering.

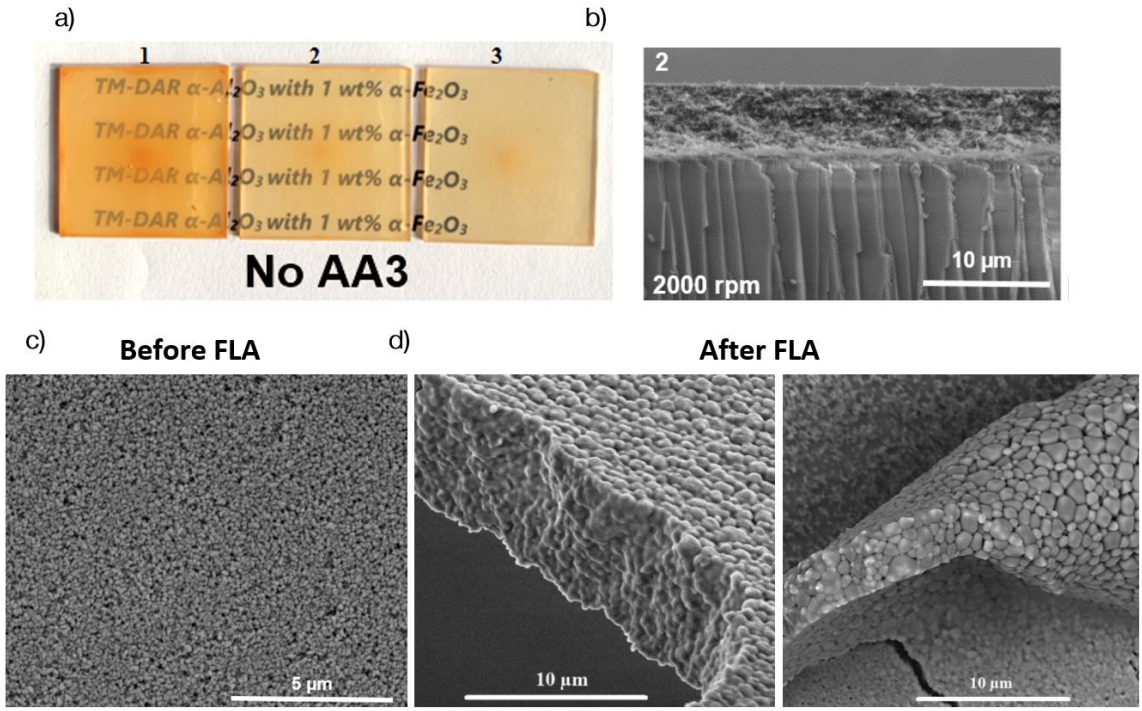

Supplementary Fig.3. Ceramic layers containing only nm-sized α-Al_2O_3 particles (no micrometer-sized AA3 particles) with α-Fe_2O_3 doping. a) Photographs of the ceramic layers spin coated with different rotation speeds (labeled 1, 2, 3), b) cross-sectional SEM image of the layer coating with 2000 rpm, c) top-view SEM images of the layers before and d) sintered after FLA (mostly delaminated or "wrapped" sintered films).

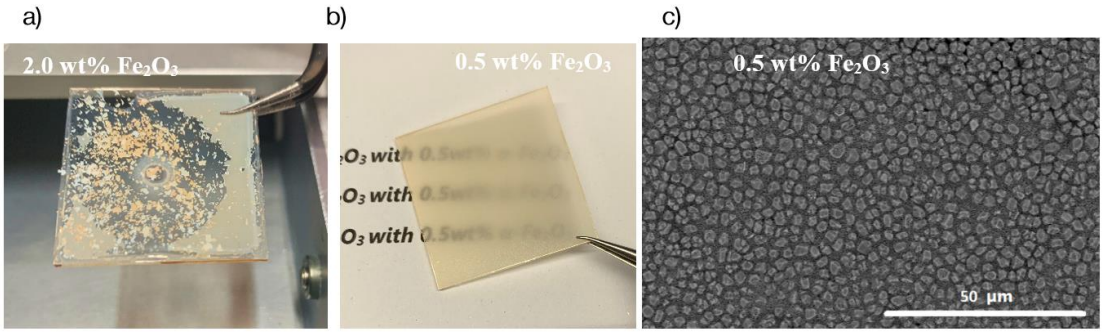

Supplementary Fig.4. Ceramic layers containing α-Al_2O_3 bimodal mixture with different amounts of the α-Fe_2O_3 dopant. Photographs of the FLA processed ceramic layers with a) 2.0 wt% and b) 0.5 wt% of Fe_2O_3 dopant. c) top-view SEM image of ceramic layer with 0.5 wt% after FLA. In the case of 2.0 wt% pulse conditions are too harsh and the samples are destroyed; for 0.5 wt% - the amount of dopant is too low and there is no effect on the layer after photonic sintering.

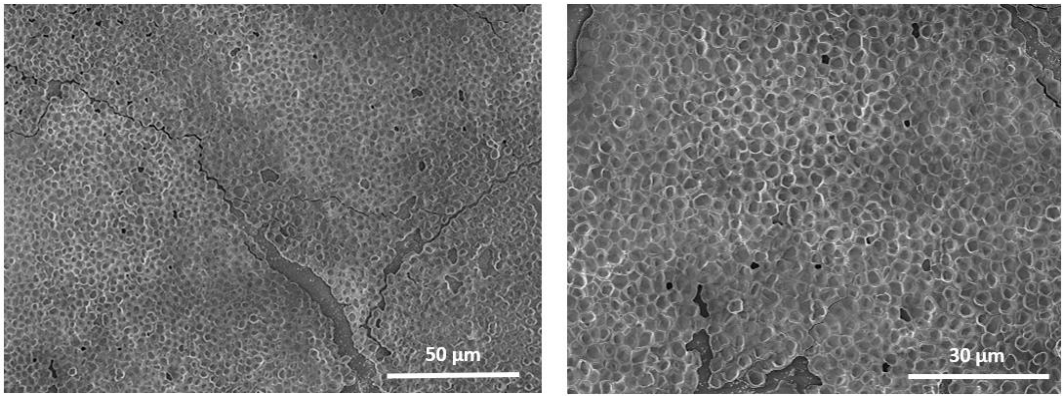

Supplementary Fig.5. Top-view SEM images of the large-area sintered layers with different magnifications.

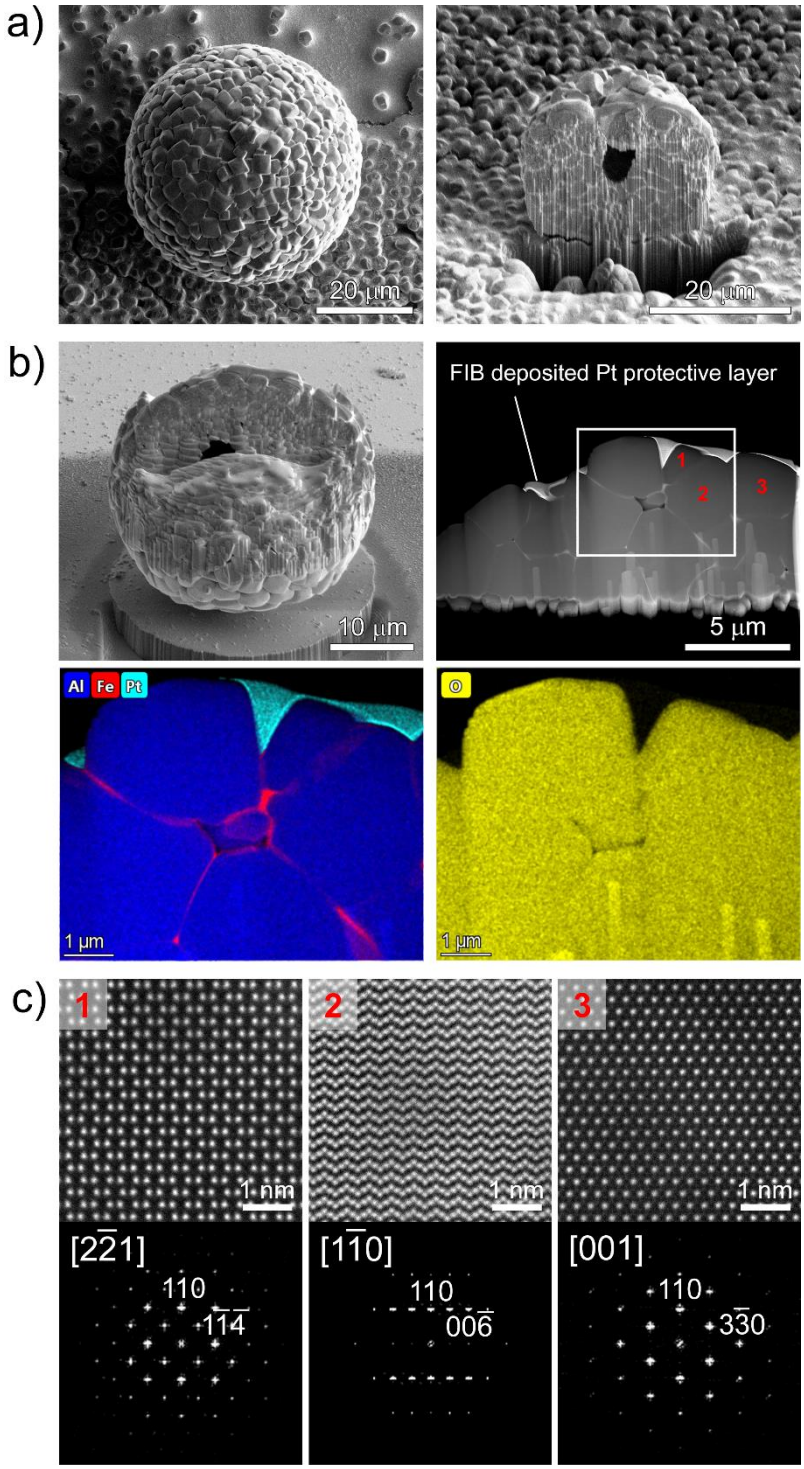

Supplementary Fig. 6. Compositional and structural analysis of the α-Al_2O_3 spheres. a, SEM images of sintered spheres (located at the edges of the sintered film). FIB cuts across the spheres reveal that they are hollow with wall thicknesses in the 3-10 µm range. b, SEM image showing the area where the FIB lamella was extracted and HAADF-STEM image of the FIB lamella. The EDX elemental maps (acquired from the white rectangle) of the FIB cross-section show the composition of the sintered sphere and the Fe localization at the grain boundaries. c, HAADF-STEM images acquired from the µm-sized α-Al_2O_3 particles indicated with 1-3 in panel b. The corresponding Fourier transforms of are all indexed using the α-phase of Al_2O_3.